

# Influence of strain rate change on corrosion fatigue behavior of A533B steel in simulated BWR water

X. Q. WU, Y. KATADA

National Institute for Materials Science, 1-2-1, Sengen, Tsukuba 305-0047, Japan  
 E-mail: wu.xinqiang@nims.go.jp

Safe operation and management in nuclear power plants require a full understanding of in-service components materials properties. Corrosion fatigue is one of the most significant corrosion-involved failures in light water reactor (LWR) plants, especially for their pressure boundary components [1]. It has been proved that the fatigue resistance of pressure vessel steels in simulated LWR coolant environments is greatly influenced by the mechanical, environmental and material factors, among which the strain rate, dissolved oxygen concentration (DO) in water and sulfur content in steels are of typical importance [2–9]. In most of previous studies the mechanical and environmental factors were usually fixed constantly throughout an individual fatigue test. Nevertheless, the above factors may vary frequently during actual operations in power plants. It is therefore necessary to investigate the influence of variation of these factors on fatigue resistance of pressure vessel steels in service environments and to develop appropriate methods for evaluating environmentally assisted fatigue damage.

The present work is to investigate the low cycle fatigue (LCF) behavior of A533B pressure vessel steel in a simulated boiling water reactor (BWR) environment. Main attention was paid on the influence of strain rate change on corrosion fatigue resistance and cyclic cracking behavior. The strain-rate dependent corrosion fatigue mechanisms are also discussed.

Hot-rolled ASTM A533B low-alloy steel plate was used in the present study. The chemical composition (wt%) was 0.17 C, 0.25 Si, 1.39 Mn, 0.003 P, 0.013 S, 0.59 Ni, 0.004 Cr, 0.46 Mo, 0.007 Co, 0.026 Al, <0.005 Cu, <0.003 V and balance Fe. The as-received microstructure was upper bainite. Round-bar specimens with 8 mm in gauge diameter and 16 mm in gauge length were machined along the rolling direction. The experimental installation was similar to that used previously [2]. LCF tests were conducted with fully reversed triangular waveform in a simulated BWR water as follows: 561 K temperature, 8.0 MPa pressure, 100 ppb DO, 6.2–6.5 pH and <0.2 μS/cm conductivity. Fatigue life  $N_f$  was defined as a number of cycles at which the peak tensile stress descended to 75% of the level of the maximum peak stress. Strain rate change tests, including the tests from a high strain rate to a low strain rate (HTL) and from a low strain rate to a high strain rate (LTH) as shown in Fig. 1, were performed. After tests, the crack morphologies on specimen surfaces were examined using a scanning electron

microscope. The number of surface long cracks (more than 500 μm in length) was counted using an optical microscope.

Fig. 2 shows the dependence of fatigue life on applied strain range in simulated BWR water. Decreasing the strain rate remarkably decreased the LCF life of A533B steel. Changing the strain rate in an individual test, i.e., both HTL and LTH, decreased the total fatigue life compared to the case at constantly high strain rate (0.1% s<sup>-1</sup>). The decrease in fatigue life closely depended on initial cycle fraction and alternate sequence

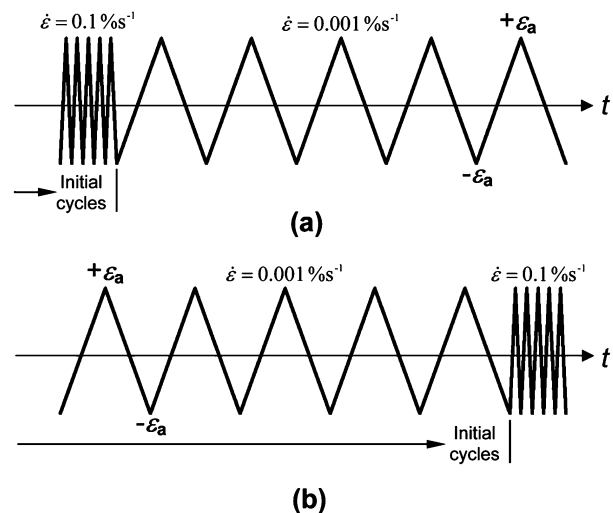


Figure 1 The strain waveforms used in: (a) HTL and (b) LTH tests.

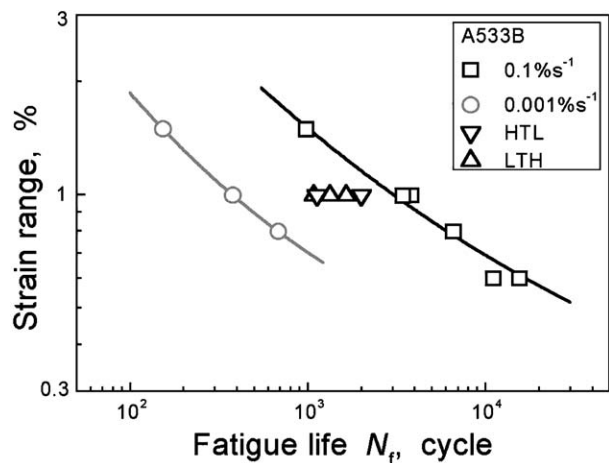


Figure 2 The dependence of fatigue life on applied strain range for A533B steel in simulated BWR water.

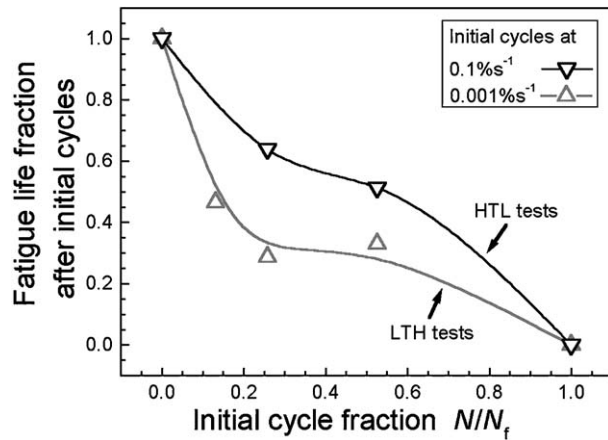


Figure 3 The influence of initial cycle fraction and alternate sequence of strain rate on following fatigue life. Here  $N$  is the number of initial cycles at a fixed strain rate,  $N_f$  is the fatigue life at this constant strain rate. Fatigue life fraction denotes the ratio between the following cycle number at another strain rate and the fatigue life at that constant strain rate.

of strain rate as indicated in Fig. 3. The larger the initial cycle fraction at low ( $0.001\% s^{-1}$ ) or high strain rate ( $0.1\% s^{-1}$ ), the smaller the fatigue life at following high ( $0.1\% s^{-1}$ ) or low strain rate ( $0.001\% s^{-1}$ ). The LTH tests showed more significant influence on fatigue life than the HTL tests.

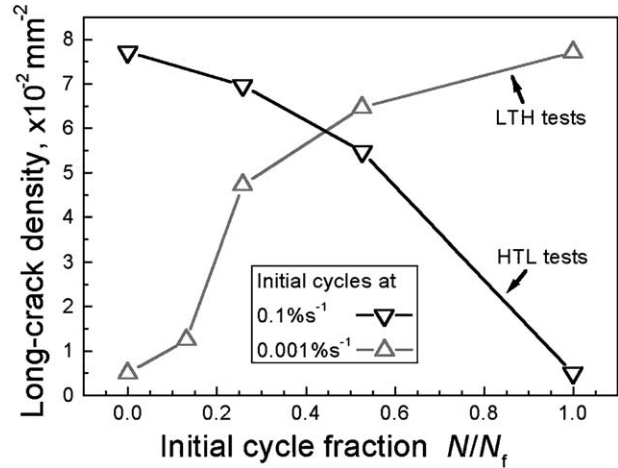


Figure 5 The relationship between surface long-crack density and initial cycle fraction. Here  $N$  and  $N_f$  are the same as those in Fig. 3.

Fig. 4 shows typical morphologies of main cracks on specimen surfaces after LCF tests in simulated BWR water. The strain rate change obviously influenced the surface crack morphologies. At high strain rate ( $0.1\% s^{-1}$ ), the main crack showed a saw-toothed or tortuous morphology and tended to grow inclined to the loading direction (Fig. 4a). At low strain rate ( $0.001\% s^{-1}$ ), the main crack showed an entirely straight morphology and grew completely normal to

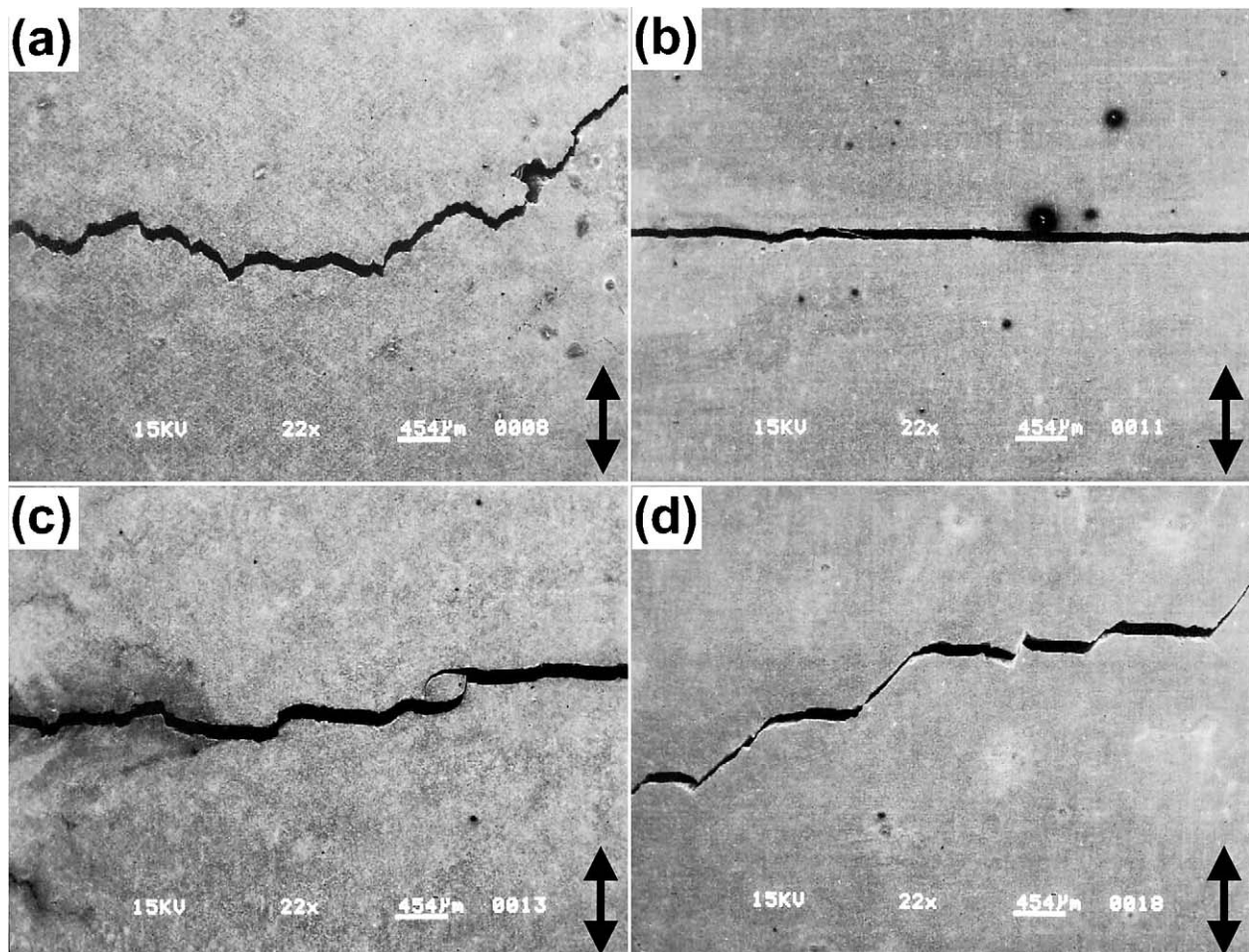


Figure 4 The morphologies of main cracks on specimen surfaces, arrows: the loading direction. (a)  $0.1\% s^{-1}$ , (b)  $0.001\% s^{-1}$ , (c) HTL test,  $N/N_f = 0.53$  and (d) LTH test,  $N/N_f = 0.53$ .

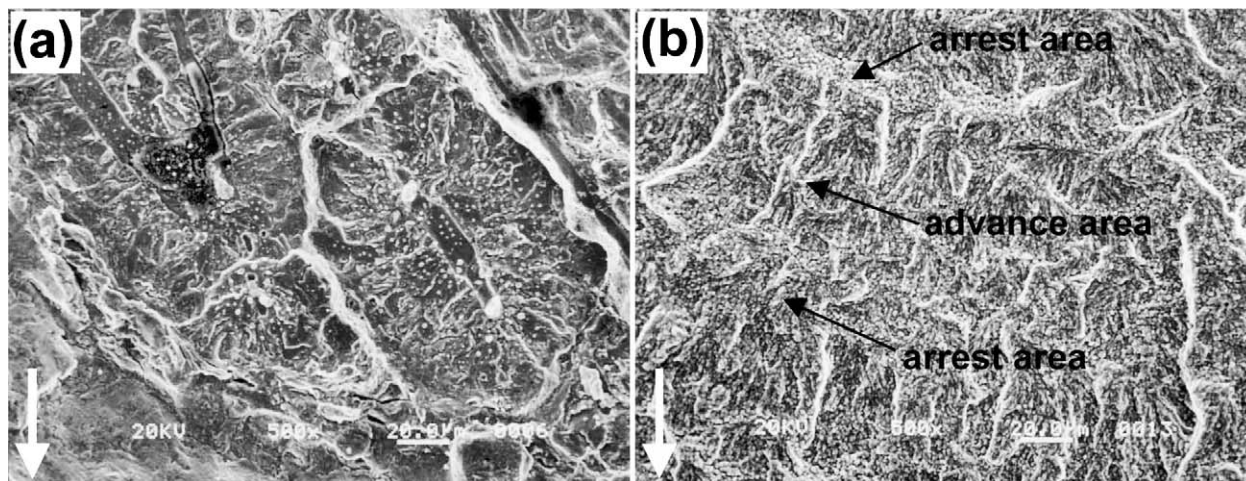


Figure 6 The fracture surface morphologies at strain rate of: (a)  $0.1\% \text{ s}^{-1}$  and (b)  $0.001\% \text{ s}^{-1}$ , white arrows: the crack growth direction.

the loading direction (Fig. 4b). A transitional cracking morphology appeared on the surfaces of specimens for both HTL and LTH tests (Fig. 4c and d).

Fig. 5 shows the relationship between surface long-crack density and initial cycle fraction at different strain rates. For the LTH tests, the long-crack density increased with increase of the initial cycle fraction at low strain rate. For the HTL tests, however, the long-crack density decreased with increase of the initial cycle fraction at high strain rate. This suggested that the initial cycles at low strain rate are more effective to initiate fatigue cracks at specimen surfaces in high temperature water than those at high strain rate.

Fig. 6 shows typical fracture surface morphologies obtained at different strain rates in simulated BWR water. In these cases the tested specimens were broken up in the liquid nitrogen and the fracture surfaces were examined. Despite being covered by oxides, distinct quasi-cleavage patterns were observed on the fracture surfaces for the case of high strain rate (Fig. 6a), while wave-like crack growth (i.e., alternate advance and arrest) was observed for the case of low strain rate (Fig. 6b).

Two distinguished cracking morphologies were observed in the present study and showed an intimate dependence on the strain rate. This strain-rate dependent cracking behavior may be attributed to a change in dominant corrosion fatigue mechanism. Up to now two basic mechanisms, i.e., hydrogen-induced cracking model and film-rupture/slip-dissolution model, have been generally proposed and accepted for interpreting corrosion fatigue behavior of pressure vessel steels in high temperature water. For the case of high strain rate, saw-toothed or tortuous fatigue cracks (Fig. 4a) were dominant and quasi-cleavage patterns (Fig. 6a) were observed on the fracture surfaces. These cracking features suggested that the hydrogen-induced cracking dominated the corrosion fatigue process, agreeing with the previous studies [9–12]. For the case of low strain rate, however, entirely straight fatigue cracks (Fig. 4b) appeared dominantly and wave-like crack growth was observed on the fracture surfaces (Fig. 6b). These cracking features were to some extent in agreement with the film-rupture/slip-dissolution model, co-

inciding with the suggestions of Chopra *et al.* [5, 13] and Scully [14]. As for the HTL and LTH tests, it was believed that a similar change in corrosion fatigue mechanism also took place corresponding to the strain rate change during the tests. The transitional cracking morphology (Fig. 4b and c) partially proved the above inference.

The change in surface long-crack density (Fig. 5) can also be rationalized by the strain-rate dependent corrosion fatigue mechanism mentioned above. At high strain rate, hydrogen-induced cracking dominated the corrosion fatigue process. Fatigue cracks preferably initiated at a few susceptible sites on the specimen surfaces such as the deep pits caused by the dissolution of MnS inclusions, the crevices between the inclusions and surrounded matrix, and so on [6, 9–12]. The surface crack density may be small due to relatively limited susceptible sites on the specimen surfaces available for the crack initiation. At low strain rate, film-rupture/slip-dissolution-induced cracking dominated the corrosion fatigue process. There was almost no limitation on crack initiation sites on the specimen surfaces. The surface crack density, thus, increased remarkably in comparison with that at high strain rate.

To sum up, the strain rate change significantly influenced the corrosion fatigue behavior of A533B pressure vessel steel in simulated BWR water. The initial cycle fraction and alternate sequence of strain rate in an individual test had important influence on the fatigue life. Distinguished crack and fracture morphologies were obtained at different strain rates. The above strain-rate dependent corrosion fatigue behavior may be rationalized by a change in dominant corrosion fatigue mechanism.

### Acknowledgments

This study was financially supported by the Budget for Nuclear Research of the Ministry of Education, Culture, Sports, Science and Technology, based on the screening and counseling by the Atomic Energy Commission in Japan. The authors also wish to thank Mr. S. Ohashi and Mr. A. Katayama in NIMS for their help in LCF tests.

## References

1. R. KILIAN and A. ROTH, *Mater. Corros.* **53** (2002) 727.
2. N. NAGATA, S. SATO and Y. KATADA, *ISIJ Intern.* **31** (1991) 106.
3. G. NAKAO, M. HIGUCHI, H. KANASAKI, K. IIDA and Y. ASADA, *ASTM STP* **1298** (1997) 232.
4. O. K. CHOPRA and W. J. SHACK, *Nucl. Eng. Des.* **184** (1998) 49.
5. *Idem.*, *J. Press. Vess. Technol. Trans. ASME* **121** (1999) 49.
6. Y. KATADA and K. KUROSAWA, *ASME PVP* **386** (1999) 249.
7. S. G. LEE and I. S. KIM, *J. Press. Vess. Technol. Trans. ASME* **123** (2001) 173.
8. A. HIRANO, M. YAMAMOTO, K. SAKAGUCHI, T. SHOJI and K. IIDA, *ASME PVP* **439** (2002) 143.
9. X. Q. WU and Y. KATADA, *ibid.* **453** (2003) 87.
10. H. HÄNNINEN, K. TORRONEN, M. KEMPPAINEN and S. SALONEN, *Corros. Sci.* **23** (1983) 663.
11. H. HÄNNINEN, W. CULLEN and M. KEMPPAINEN, *Corrosion* **46** (1990) 563.
12. J. D. ATKINSON and J. YU, *Fat. Fract. Eng. Mater. Struct.* **20** (1997) 1.
13. D. J. GAVENDA, P. R. LUEBBERS and O. K. CHOPRA, *Fat. Fract. J.* **350** (1997) 243.
14. J. C. SCULLY, *Corros. Sci.* **20** (1980) 997.

*Received 30 September  
and accepted 29 October 2003*